Manuscript received July 4, 2007; revised Oct. 17, 2007

Limitations of Current 4G Systems and Its Substitute Schemes with TDD/TDMA

LU ZHAOGAN, ZHANG TAIYI, SHEN XIAODONG, LI XIAOHE
School of Electronic & Information Engineering, Xi'an Jiaotong University, CHINA
Email: luzhaogan@mailst.xjtu.edu.cn

Abstract: - In current 4G system given in recent literatures, channel estimation overhead and complexity of multi-user detectors (MUD), may lead to bad performance in fast fading channel scenarios when large number of users exists. So, a novel 4G system with TDD/TDMA as duplex and wireless access is designed to reduce channel estimation spending and avoid MUD, as only one user can be active to communicate with base station. Under the requirement of 4G systems, radio frame structure is elaborately designed to fit for fast fading channel scenarios. Construction of training sequences for channel estimation is also detailed together with a novel eigenmodes coupled universal space-time codes. The system architecture with consideration of link adaptations is given and evaluated for performance of TDD/TDMA 4G systems. Results show the proposed TDD/TDMA 4G can meet the requirement of 4G system under the classical ITU channel profiles.

Key-word: - MIMO, OFDM, orthogonal eigenmodes, 4G, link adaptation

1 Introduction

Since the third-generation (3G) wireless mobile communication networks was deployed throughout the world, the designs of 3G beyond or the fourth-generation (4G) wireless communications systems under frequency selective fast fading channel scenarios, has recently attracted a lot of attention. Multiple-input multiple-output (MIMO) architectures [1-2] are very attractive solutions for high date rate wireless communication systems due to their enormous potential for capacity gains relative to single-antenna systems. Furthermore, orthogonal frequency-division multiplexing (OFDM) [3-4] is one of the most promising techniques to realize the high bit-rate transmission, because OFDM is a multi-carrier transmission scheme with a guard interval (GI), and can maintain excellent transmission performance even in multipath fading channels. So, many design schemes based MIMO and OFDM were given by recent literatures [5-14], such as VSF-OFCDM by DoCoMo Japan [5-7], TDD-MIMO-OFDM by FuTURE project of China [8-11], TDD-CDM-OFDM as the evolved version of TD-SCDMA by Datang Mobile [12-14], and so on.

However, code-division multiple access (CDMA) or orthogonal frequency-division multiple access (OFDMA) are adopted by these 4G schemes, although it is necessary to keep stable evolution between different communication systems. When multiple user terminals equipped with multiple transmit antennas, two intractable issues are caused, i.e., channel estimation bandwidth overhead and complexity of multiple user detectors (MUD). According to channel estimation theory [15-18], the length of training sequences in time domain and frequency domain are at least Mt times that of channel profiles or the number of carrier tones respectively, where *Mt* denotes the number of transmit antennas. For the scenarios with many users simultaneously communicating with base stations (BS), the length of pilot sequences will increase proportionally with the number users in current covering areas. In frequency fast fading wireless channels, channel information must be frequently estimated by transmitting pilot sequences in smaller intervals than that for slow fading channel environments. Thus, the bandwidth overhead of channel estimations will be the main appropriator of channel resources, subsequently decreases spectrum efficiency. Another problem is the proportionally increasing complexity of MUDs with the numbers of users and their transmit antennas, as every transmit antenna at terminals can be regarded as one user with single transmit antenna. As the increase of users, the MUDs will be badly effected by the interference of signals from different transmit antennas at different user terminals. Furthermore, the increasing complexity of MUD can also limit its application in practical cases.

In order to get rid of such problems, we design a novel 4G mobile communication system with time division duplex (TDD) and time divisions multiple

access (TDMA). Based on MIMO and OFDM technology, the 4G scheme with 20MHz bandwidth can reduce channel estimation overhead and avoid MUD as only one user can communicate with BS at a time. However, efficient scheduling algorithms must be conducted to allocate corresponding bandwidth resources to different users in the proposed TDD/TDMA 4G system. For the limitation of length, this paper only considers PHY design and its implementation scheme, and other design of TDD/TDMA 4G systems will be studied in subsequent research.

This paper is organized as follows. According to the channel scenarios where the proposed TDD/TDMA 4G systems work, some configuration parameters are determined in Section 2 along with their structures of wireless frame, synchronization slot and the Stainer channel estimation methods. Subsequently, link adaptation about eigenmodes and power allocation scheme are detailed and then followed by the implementation frame of TDD/TDMA 4G systems in section 3. Then, section 4 details the system architecture of TDD/TDMA 4G systems. Finally, in section 5, system capacity and performance in terms of bit error rates are evaluated by Matlab Simlink tools and conclusions are presented in Section 6.

2 PHY Design

The target frequency band for this system is 2–5 GHz due to favorable propagation characteristics and low radio frequency (RF) equipment cost. The broadband channel is typically non-LOS channel and includes impairments such as time-selective fading and frequency-selective fading. According to technical requirements of the broadband cellular channel and constraints of practical of hardware and RF, the PHY design of TDD/TDMA 4G systems is given in following.

2.1 Design Parameters

The time interval of channel estimation and the subcarrier separation for multiple-carrier transmission are determined by coherence time and bandwidth of wireless channels, respectively. So, coherence time and bandwidth of target channels for TDD/TDMA 4G systems, is firstly determined in followings. As the proposed TDD/TDMA 4G systems can fit for target cellular channel scenarios, we consider the typical multi-path fading propagation conditions [19] as target scenarios, and use the ITU Vehicular Channel Models (channel B) [19] as target cellular channels.

According to the tapped-delay-line parameters of the ITU Vehicular Channel (channel B), which has maximum root mean square delay τ_{rms} = 4000ns, its coherence bandwidth (B_c) can be achieved by [20]

$$B_c = \frac{1}{5\tau_{rms}} = 50\text{kHz} \quad (1)$$

For mobile stations (MS) with 500km/h, the channel coherence time (T_c) is calculated by its corresponding Doppler frequency (f_d =924.3Hz) [20], i.e.

$$T_c = \sqrt{\frac{9}{16\pi f_d^2}} = 1.07\,\text{ms} \quad (2)$$

As pointed out in literature [21], it is suitable to take one third of coherence bandwidth (B_c) as subcarrir frequency spacing, for the reasons of complexity of FFT for small frequency spacing and poor peformance for large frequency spacing. Firstly, guard time (T_G) is taken as four times the root mean square delay of cellular channels, i.e., T_G =16us. Subsequently, the length of OFDM symbols (T_s) is taken as five times that of guard time, i.e. $T_s = 80$ us. So, subcarrier spacing (Δf) is given as

$$\Delta f = \frac{1}{T_s - T_G} = 15.625\,\text{kHz} \quad (3)$$

Then, the 20MHz bandwidth can be divided into 1280 sub-channels rather than the number of 2 integer power. In order to efficiently implement FFT, carrier number (N) is assumed to 2048, and the subcarrier spacing is finally given as

$$\Delta f = \frac{B}{N} = 9.765625\,\text{kHz} \quad (4)$$

where B denotes channel bandwidth (B=20MHz).

In practical OFDM systems, many sub-carriers are used as guard bands and DC carrier to keep interference from other systems. If carrier spacing is taken as 9.765625 kHz, many sub-carriers could not be utilized completely. So, in order to increase spectrum efficiency, carrier spacing should be larger that given in (4). Here, the carrier spacing for 802.16a wireless local networks [22], is taken as the carrier spacing of TDD/TDMA 4G systems, i.e., $\Delta f = 11.16$ kHz, which is much smaller than the coherence bandwidth as showed in (3). The first 127 and last 128 sub-carriers are used as lower frequency and higher frequency guard bands respectively, and DC carrier is reserved. The residual 1792 sub-carriers are used to transport data symbols, completely, without pilot symbols inserted into fixed sub-carriers.

2.2 Frame Structure

In order to meet the requirement [23] of fast beam forming in high moving speed as 120km/h when the smart antenna technology is deployed, the length of radio sub-frame is taken as 5ms similar to that of TD-SCDMA radio sub-frame, other than 10ms in WCDMA/TDD systems.

As shown in Fig.1, a radio frame with duration of 5 ms is subdivided into 7 main time slots (TS) of 675 μs duration each and four special time slots: down link synchronization (DwPTS), switch slot from down links to up links (TTG slot), up link synchronization (UpPTS), and switch slot from up links to down links (RTG slot). Time slot TS0 is always used for down links, whereas the other time slots can be used for either up links or down links, depending on flexible switching point configuration. The location information about TTG Slot, UpPTS and switch points would be sent to mobile stations by information transported in TS0. As the synchronization slot for down links, DwPTS can calibrate the synchronization between BS and MS, estimate and compensate carrier frequency offset due to frequency drift of carrier generators at transmitter and receivers. So does the UpPTS for up links. Due to the requirement of synchronization accuracy of timing and carriers, their durations are determined to 75us so that BS and MS can achieve the same synchronization performance. For systems with TDD, switch slots between up links and down links should be greater than the maximum round time of radio between transmitter and receivers, that is double of the maximum radio delay profiles [22]. According to the profiles of the ITU Vehicular Channel (channel B), after refering to frame structure in 802.16a TDD [22] and inital frame struacture in TD-SCDMA [24], the durations for TTG and RTG is 75us and 50us, respectively, under the limation of the 5ms radio sub-frame length.

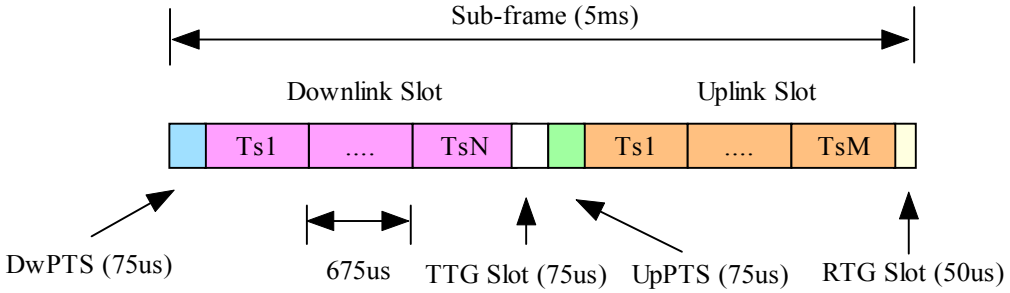

Fig.1 Frame structure of TDD/TDMA 4G systems with 7 data time slots, 2 synchronization slots and 2 switch slots for up links and down links.

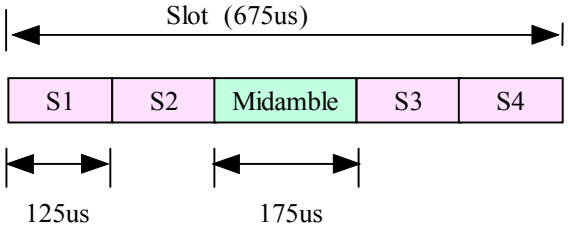

Fig.2 Burst structure of TDD/TDMA 4G systems, where Midamble is training sequence for channel estimation in time domain and the estimated channel information is used to decoding data symbols before and after Midamble.

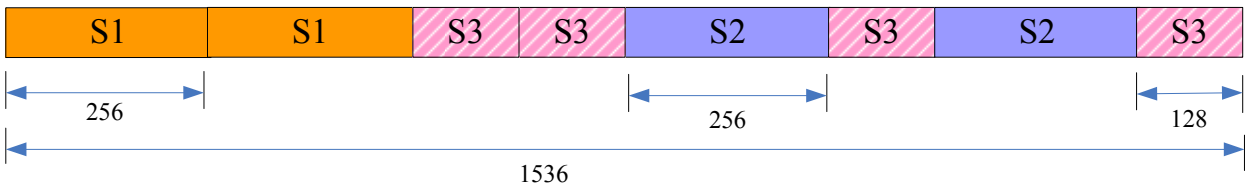

Fig.3 Structure of synchronization slot for TDD/TDMA 4G systems, where timing synchronization and fine-coarse carrier frequency synchronization can be done by identical training sequences distributed in different intervals.

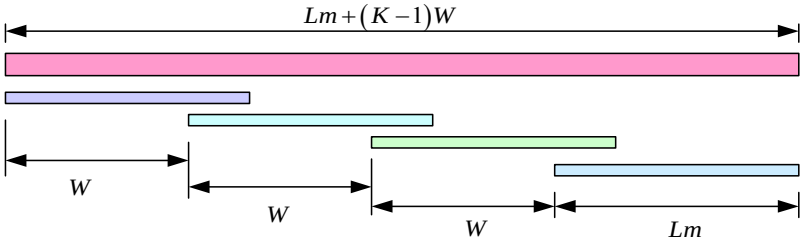

Fig.4 Construction of Midamble by truncating the circular extended version of a basic sequence.

2.3 Burst Structure

The burst structure of the data time slots consists of 4 data blocks and 1 training signal for channel estimation in time domain, as showed in Fig.2. Actually, one data block is one MIMO OFDM symbol, whose duration is 125us, while midamble is the training symbols for channel estimations in time domain and the estimated channel information is used to decode data symbols before and after midamble codes. The sample rate of IFFT/FFT for data blocks is 20.48MHz.

2.4 Synchronization Slots

In proposed TDD/TDMA 4G systems, links between BS and MS are actually equivalent to point to point links, so synchronization slots for up links and down links have the same slot structures and consist of 1536 samples. According to the strategies [25-26] for timing synchronization and carrier frequency offset estimation, a novel synchronization slot is designed to conduct timing synchronization and the fine and coarse carrier frequency offset estimation through identical training sequences distributed in different intervals, as displayed in Fig.3.

Firstly, two identical training sequences S1 transmitted in series by transmitters are used to obtain coarse timing synchronization by calculating the delay correlation function of training sequences. Subsequently, fine timing synchronization is done through two training sequences S3. Furthermore, the conjoint two S3 have small time delay with large frequency offset estimation range, and can be also used to conduct coarse frequency offset estimation. Then, different delay S2 and S3 have large delay with small frequency offset estimation range and are used to perform fine frequency offset estimation by averaging their estimated frequency offsets.

2.5 Stainer Channel Estimation

As showed in section 2.3, the midamble symbols are used to conduct channel estimation and track channel fluctuation information, and both data symbols before and after midamble can be checked out according the estimated channel states by midamble. Compared with FuTURE B3G TDD systems [8-11], channel estimation overhead is reduced greatly with simple implementation. The midamble code with duration about 175us consists of 3585 samples, and is obtained by truncating the circular extended version as showed in Fig.4.

Denote *Lm* as length of training sequence, *W* as length of spatial channel impulse respondence, and L = W*Mt as length of a basic sequence, which can be delineated as

$$\mathbf{m} = \left(m_1, m_2, ..., m_L\right) \tag{5}$$

Its circular extension version is given by

$$\bar{\mathbf{m}} = \left(\bar{m}_1, \bar{m}_2, ..., \bar{m}_{L_m+(M_t-1)W}\right) \tag{6}$$

where the first L elements are consistent with corresponding elements of the basic sequence and other elements are determined by

$$\bar{m}_i = m_{i-L}, \ \ i = \left(L+1\right), \cdots, \left\lceil L_m + \left(M_t - 1\right)W \right\rceil \tag{7}$$

Then, training sequences for different transmit antennas are obtained by truncating the circular extended version. Furthermore, the pilot for the *u*-th transmit antenna is presented as

$$\mathbf{m}^{(u)} = \left(m_1^{(u)}, m_2^{(u)}, ..., m_{L_m}^{(u)}\right) \tag{8}$$

where

$$m_i^{(u)} = m_{i+(M_t-1)W}, \ \ i = 1, ..., L_m, \ \ u = 1, ..., M_t \tag{9}$$

If the design parameters showed above can be denoted as a quaternion (L_m,L,M_t,W), there exists the following relationship among these parameters, i.e.,

$$W = \left\lfloor \frac{L_m}{M_t + 1} \right\rfloor, \ \ L = WM_t \tag{10}$$

where operator $\lfloor \cdot \rfloor$ denotes the largest integer not more than a given real number in the operator.

However, the training sequences given by (8) are generally described as binary sequences, and should be converted into complex number. Firstly, they are re-presented as bi-polar sequences and then further converted into complex numbers. Denote $\vec{\mathbf{m}}^{(u)}$ as one bi-polar sequence, $\mathbf{m}_c^{(u)}$ as its correspondent complex form, which can be

determined by

$$m_c^{(u)}(i) = \left(j\right)^i \cdot \vec{m}^{(u)}(i), \quad i = 1,...,L \tag{11}$$

where j is unit of imaginary number.

It is the elaborately designed training symbols as showed above, that result in the circular pilot matrix. So, the pilot sequence pilot design scheme can avoid matrix inversion calculation, and the complexity of MIMO channel estimation can be further reduced.

3 Link Adaptations

3.1 Eigenmodes with Space-Time Codes

Firstly, a universal space-time code can be defined as a rate *T/K* Mt×K design scheme over a complex subfield ***A*** of the complex field $\mathbb{C}$, whose codeword matrix ***X*** is a Mt×K matrix with entries obtained from the *K*-linear combinations of *T* data symbols and their conjugates. If a codeword matrix ***X*** is represented as a column vector by stacking its columns, the column vector can be delineated as the linear transform of *T* data symbols and their conjugates, i.e.,

$$vec\left(\mathbf{X}\right) = \mathbf{\Phi s} \tag{12}$$

where $vec(\cdot)$ denotes the column vector by stacking the columns of a matrix into one column vector, ***s*** is a column vector whose elements consist of *T* data symbols and their conjugates, and the transform matrix $\mathbf{\Phi}$ is denoted as the *generation matrix* of the space-time code design scheme.

The least squared estimation of ***s*** can be achieved as following

$$\hat{\mathbf{s}} = \left(\tilde{\mathbf{H}}\mathbf{\Phi}\right)^{-1} vec\left(\mathbf{y}^T\right) + \hat{\mathbf{w}} \tag{13}$$

where $\hat{\mathbf{w}} = \left(\tilde{\mathbf{H}}\mathbf{\Phi}\right)^{-1} vec\left(\mathbf{w}^T\right)$, $\mathbf{y}$ is the received signal matrix whose rows are the received data symbols polluted by channel fading and noise at every receive antennas, $\mathbf{w}$ is the corresponding noise of $\mathbf{y}$, $\hat{\mathbf{s}}$ denotes the estimation version of ***s,*** and $\tilde{\mathbf{H}}$ is the equivalent channel matrix assembled by fading coefficients at different carriers for different spatial links.

Let $\bar{\mathbf{H}} = \tilde{\mathbf{H}}\mathbf{\Phi}$, it can be decomposed into orthogonal eigenmodes by singular value decomposition as showed

$$\bar{\mathbf{H}} = \mathbf{UDV}^H \tag{14}$$

where ***U*** and ***V*** denote the unitary matrices representing the left and right eigenvectors of $\bar{\mathbf{H}}$, respectively, and ***D*** is a diagonal matrix, whose elements are the ordered singular values of $\bar{\mathbf{H}}$, i.e., the corresponding fading coefficients of those orthogonal eigenmodes .

Then, substituting $\bar{\mathbf{H}}$ by its SVD, we can get

$$\mathbf{U}^H vec\left(\mathbf{y}^T\right) = \mathbf{DV}^H\mathbf{s} + \mathbf{U}^H vec\left(\mathbf{w}^T\right) \tag{15}$$

Now, let $\mathbf{y}' = \mathbf{U}^H vec\left(\mathbf{y}^T\right)$, $\mathbf{s}' = \mathbf{V}^H\mathbf{s}$, $\mathbf{w}' = \mathbf{U}^H vec\left(\mathbf{w}^T\right)$, and (15) can be rewritten as

$$\mathbf{y}' = \mathbf{Ds}' + \mathbf{w}' \tag{16}$$

Furthermore, it is also equivalent to

$$\begin{cases} y_i' = \sqrt{\lambda_i}s_i' + w_i' & \left(i = 1,2,\cdots,r\right) \\ y_i' = w_i' & \left(i = r+1, r+2,\cdots,m\right) \end{cases} \tag{17}$$

where r and $\sqrt{\lambda_i}$ are the rank of $\bar{\mathbf{H}}$ and its i-th singular value, respectively.

3.2 Improved Water-Filling Power Allocation

Based on adaptive modulation margin adaptive (MA) principals [27], link adaptation techniques can be implemented from two aspects, i.e., adaptive power allocation under total transmit power constraint for maximal transported bits, and adaptive bits allocation under total transmit bits for minimal transmit power, respectively. Under the constraints of given total power and target bit error ratio (BER), we only consider how to conduct power allocation to orthogonal eigenmodes to maximize transmit bits.

In order to maximize the transported total bits, an improved water-filling power allocation scheme is given on the base of classical water-filling schemes. According to the scheme, the adaptive power and bit allocation are conducted in two steps. Firstly, an initial power allocation is given by classical water-filling scheme, That is, the first step is executed to initially allocate the power for different orthogonal eigenmodes according to the classical water-filling scheme. Then, after determining the transported bits at channel eigenmodes, the residual power is reallocated among these eigenmodes to transport additional bits.

For given target BER P_e, the transmit power for an additive white Gaussian noise (AWGN) channel to transmit *c* bits information with M-QAM modulation, is given by [11]

$$P\left(c\right) = \frac{\sigma^2}{3}\left[Q^{-1}\left(\frac{P_e}{4}\right)\right]^{-2}\left(2^c - 1\right) \tag{18}$$

Where $Q(x) = \frac{1}{2\pi}\int_x^\infty e^{-t^2/2}dt$ is denoted as complementary error function. Then, for given transmit power, the number of bits transported by the AWGN channel, can be derived according to (18), as showed in the following formula

$$c = \text{floor}\left[\log_2\left(1+\frac{3P}{\sigma^2}\left(Q^{-1}\left(\frac{P_e}{4}\right)\right)^2\right)\right] \quad (19)$$

where *floor* denotes the operator to round towards minus infinity.

Now, we present the details of the improved water-filling scheme, which is conducted in tow steps as showed in followings.

1. Initial power allocation based water-filling scheme

For the eigenmodes given by (17), the power allocation scheme can be described as an optimal problem to maximize the system capacity under the constraint of given total transmit power, i.e.,

$$C_{\max} = \max_{P_i(i=1,\cdots,r)} \sum_{i=1}^{r} \log_2\left(1+\frac{P_i\lambda_i}{\sigma^2}\right) \text{ st.} \sum_{i=1}^{r} P_i = KP \quad (20)$$

where C denotes system capacity, while P is the given total transmit power. According to water-filling power allocation algorithm, the optimal power allocation can be given by

$$P_i = \max\left(0, \mu - \frac{\sigma^2}{\lambda_i}\right) \quad (i=1,2,\cdots,r) \quad (21)$$

where $\mu = \frac{1}{r}\left(KP + \sum_{i=1}^{r}\frac{\sigma^2}{\lambda_i}\right)$, and σ^2 is noise variance of orthogonal eigenmodes , assumed to have the same variance.

The power allocated to orthogonal eigenmodes as showed in (21), is called *water-filling power* to distinguish different power allocation results in the following. With the *water-filling power* allocated *i*-th eigenmode, its maximal bits carried can be given by (13), that is

$$c_i = \text{floor}\left[\log_2\left(1+\frac{3P_i}{\sigma^2}\left(Q^{-1}\left(\frac{P_e}{4}\right)\right)^2\right)\right], (i=1,2,\cdots,r) \quad (22)$$

However, according to (18), the necessary power to transmit c_i bits is determined by

$$\tilde{P}_i = \frac{\sigma^2}{3}\left[Q^{-1}\left(\frac{P_e}{4}\right)\right]^{-2}\left(2^{c_i}-1\right), \quad (i=1,2,\cdots,r) \quad (23)$$

which is called the *expectation power* to transmit c_i bits. Clearly, the *water-filling power* for *i*-th eigenmode is larger than its *expectation power*, and their difference is named as *residual power*, which will be further reallocated among these eigenmodes.

2. Reallocation of residual power

Subsequently, on the basis of the power allocation results in the first period, we calculate the additional power to transmit an additional bit at *i*-th eigenmode. That is,

$$\Delta\tilde{P}_i = \left[P(c_i+1) - P(c_i)\right]/\lambda_i^2, \quad (i=1,2,\cdots,r) \quad (24)$$

which is called *additional power*. Then, an *accumulative sum sequence* is obtained by a sorted version of *additional power* in ascending order at all the eigenmodes. The elements in the *accumulative sum sequence*, not more than the *total residual power*, can be found out, and the eigenmodes corresponding with these elements can transport an additional bit. So, the *additional powers* of these eigenmodes are allocated to these eigenmodes from the *total residual power*, whose residual power after reallocation, i.e., *total overplus power*, is averagely allocated to all the eigenmodes. At last, the bit number of these eigenmodes should be increased by one, respectively.

4 System Architectures

Considering a TDD/TDMA 4G systems with two and eight antennas at MS and BS, its system architecture is designed as showed in Fig.5, where the simplified block diagrams of MS and BS are given in Fig.5(a) and Fig.5(b), respectively. Furthermore, adaptive modulation and codes (AMC), adaptive power control (APC) and adaptive space time codes (ASTC) are used to conduct link adaptation with eigenmodes detailed in section 3.1. Compared with DoCoMo 4G [5-7] and FuTURE TDD [8-11], the proposed TDD/TDMA 4G systems have smaller carrier bandwidth and simple implementation, and can fit for larger cell area with fast fading channel scenarios. What's more, the configuration with 2x8 antennas at MS and BS could also make TDD/TDMA 4G system serve as an evolution version of TDS-CDMA 3G system [12-14] , proposed by Datang Mobile. Their system configuration could be found in Tab.1.

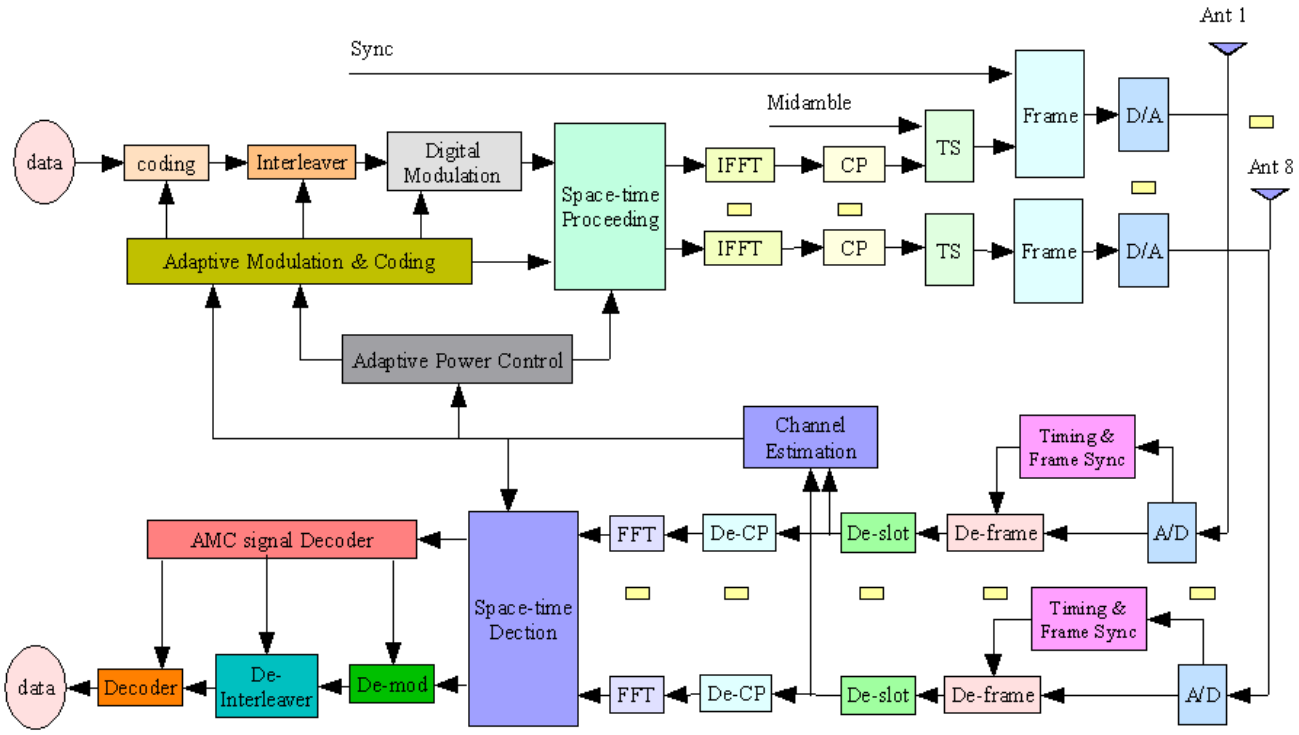

(a) Block Diagram of BS

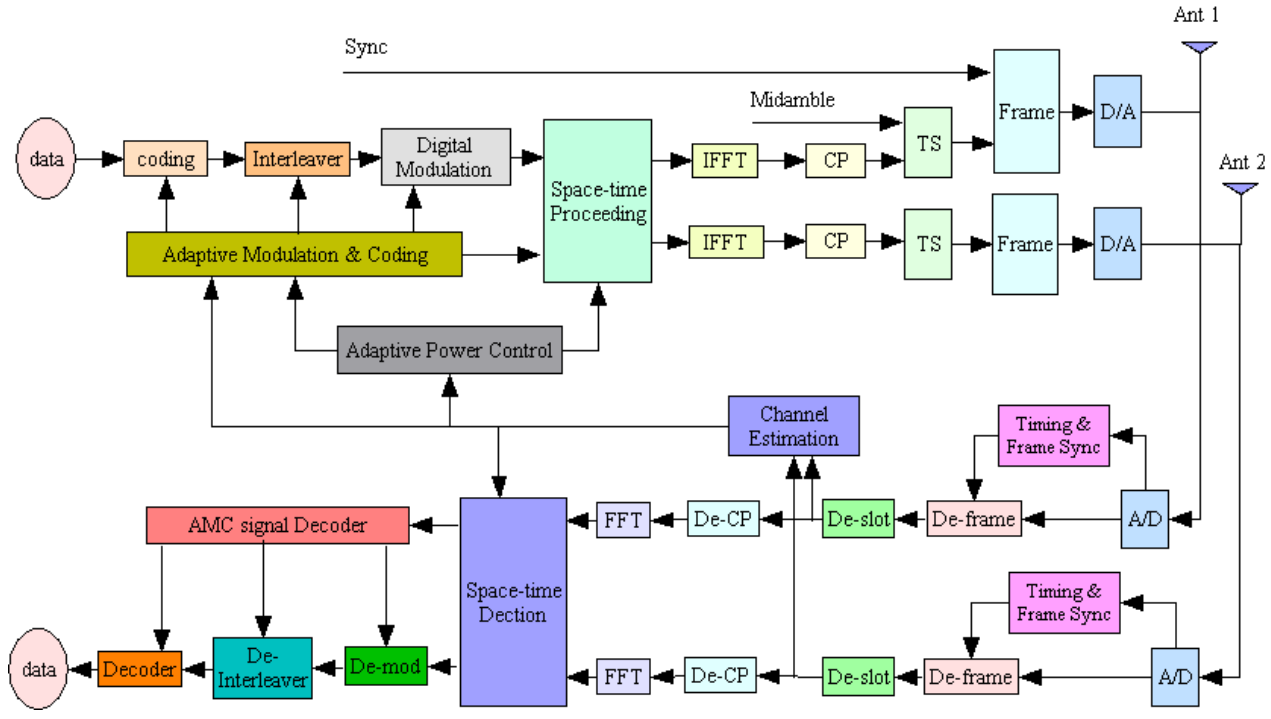

(b) Block Diagram of MS

Fig.5 System Architecture of TDD/TDMA 4G System

Tab.1 System Configuration of TDD/TDMA 4G, DoCoMo 4G and FuTURE TDD

	TDD/TDMA 4G	DoCoMo 4G		FuTURE TDD
		VFS-OFDM (Downlink)	MC/DS-CDMA (Uplink)	
FFT/IFFT Sample Rate	20.48Msps	135Msps	--	24.15Msps
Carrier Frequency	2GHz	4.635GHz	4.9GHz	3.5GHz
Chip Rate	--	--	16.384Mcps	--
FFT Size	2048	1024	--	1024
Carrier Bandwidth	11.16kHz	131.836 kHz	20 MHz	19.5kHz
Number of Low Frequency Guard Sub-carrier	127	127	--	69
Number of High Frequency Guard Sub-carrier	128	128	--	70
Number of Pilot Sub-carrier	0	0	--	52
Number of Data Sub-carrier	1792	768	2	832
Cyclic Prefix Duration (us)	25	1.674	--	10.6
Symbol Duration (us)	125	9.259	--	53
Length of Radio Frame (ms)	5	0.481 (48 Data + 4 Pilot symbols)	0.5	5
Bandwidth	20MHz	100MHz	40 MHz	20MHz
Antenna Configuration	2x8	2x4	2x4	2x8
Number of Sub-carrier	2048	1024	2	1024
Wireless Access	TDMA	CDMA	CDMA	TDMA/OFDMA
Duplex	TDD	FDD		TDD

5 Performance Evaluations

In this section, system capacity of the proposed TDD/TDDMA 4G systems without and with link adaptation is numerically evaluated. Furthermore, their throughout and bit error ratio (BER) is also simulated through Matlab 7.0 simulink blocksets.

5.1 Capacity of TDD/TDMA 4G Systems

The outage capacity of TDD/TDMA 4G systems for outage probability of 0.1 is evaluated under the ITU indoor and vehicle channel scenarios [19] with velocity of 250km/h and 500km/h, as showed in Fig.6. According to the results indicated by Fig.6, the OFDM technology can convert frequency selective channels into flat fading sub-channel, which have approximate system spectrum efficiency as that of flat fading systems. Furthermore, the system capacity of TDD/TDMA 4G systems in up links is similar to that in down links, and this can owe to the coupled MIMO with OFDM technology, which can fit bad wireless channel conditions.

At the signal noise ratio (SNR) of 25dB with 20MHz bandwidth, the outage capacity for outage probability of 0.1 can achieve to 400Mbps, enough for the requirement of data transmission rate 100Mbps under indoor scenarios.

5.2 System Capacity with Adaptive Transmit Power Allocation

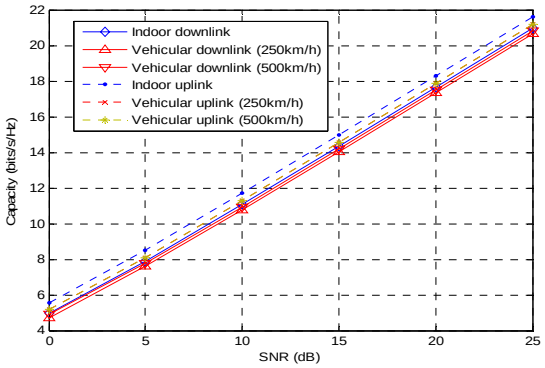

Fig.6 Outage Capacity of TDD/TDMA 4G System for Outage Probability of 0.1

When the channel state information (CSI) is known at the transmitter, the capacity can be increased by assigning the transmitted power to various antennas according to the "water-filling" rule [28]. It allocates more power when the channel is in good condition and less when the channel state gets worse.

Figs.7 and Fig.8 show the capacities estimated by simulation of an adaptive and a no adaptive system, for a number of receive antennas as a parameter and a variable number of transmit antennas over a Rayleigh MIMO channel, at an SNR of 25 dB. In the adaptive system the transmit powers were allocated according to the water-filling principle and in the no adaptive system the transmit powers from all antennas were the same. As indicated in Fig.7 and Fig.8, when channel state

information are known at both transmitter and receiver, the capacity of TDD/TDMA 4G systems can achieve to 20bits/s/Hz, with adaptive transmit power allocation between different eigenmodes .

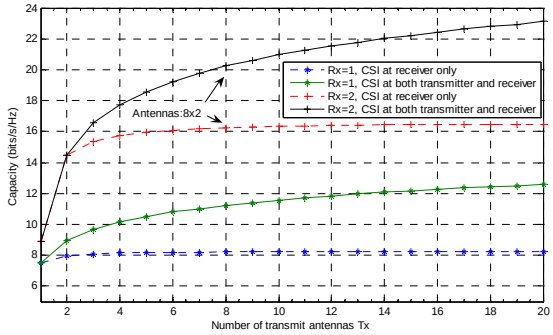

Fig.7 Achievable capacities for adaptive and no adaptive transmit power allocations over a fast MIMO Rayleigh channel, for SNR of 25 dB, the number of receive antennas $n_R = 1$ and $n_R = 2$ and a variable number of transmit antennas

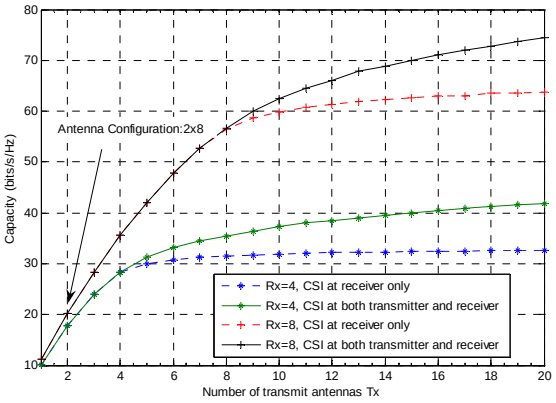

Fig.8 Achievable capacities for adaptive and nonadaptive transmit power allocations over a fast MIMO Rayleigh channel, for SNR of 25 dB, the number of receive antennas $n_R = 4$ and $n_R = 8$ and a variable number of transmit antennas

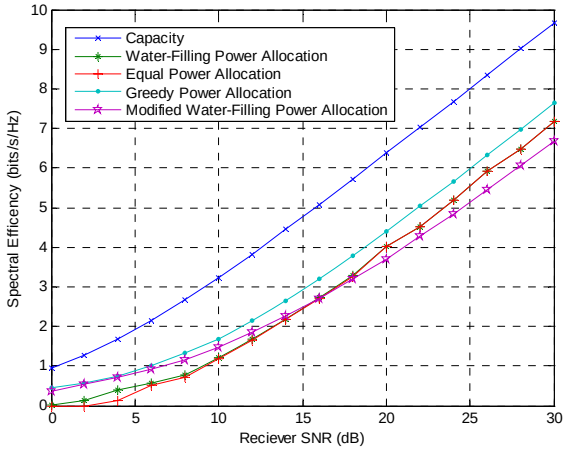

Fig.9 Spectrum Efficiency of Different Power Allocation Schemes for single antenna OFDM system

5.3 System Performance of Link Adaptation

In order to evaluate performance of TDD/TDMA 4G systems with link adaptation, classical water-filling scheme [29], greedy scheme [27], equal power allocation [30] and the scheme given in this paper are firstly numerically simulated in the case of single antenna scenarios, and Fig.9 discloses their compared results. When the SNR at receiver is lower than 15dB, the modified water-filling power allocation algorithm can achieve better performance than that of classical water-filling scheme and equal power allocation schemes, but inferior to that of greedy power allocation scheme. However, different from greedy scheme, the modified water-filling power allocation method is conducted in only two steps.

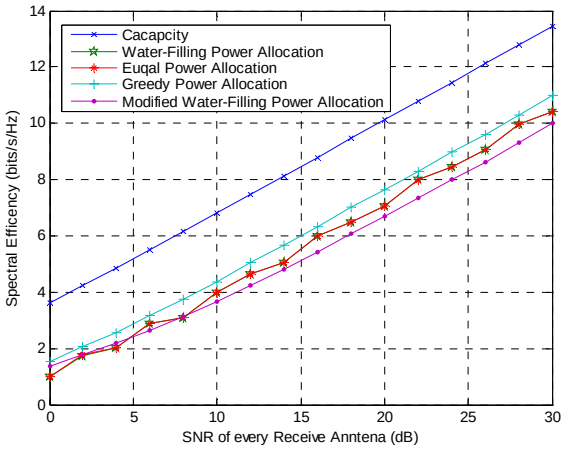

Fig.10 Spectrum Efficiency of TDD/TDDMA 4G System under different power allocation schemes

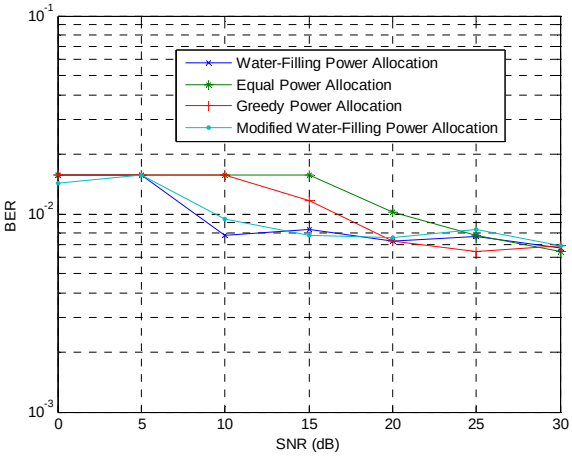

Fig.11 System BER of TDD/TDMA 4G Systems with Different Power Allocation

Subsequently, according to CSI at transmitter, transmit power is firstly adaptively allocated among different eigenmodes as detailed in section 3.1,

then AMC and ASTC are performed to fit for current channel states for given special BER requirements. The four different power allocation strategies as showed above are used to conduct adaptive power allocation. Fig.10 shows the system spectrum efficiency achieved by different power allocation schemes, and the spectrum efficiency of modified water-filling scheme is inferior to that of other three schemes at high SNR, as great diversity gain can be achieved under the case of TDD/TDMA 4G systems. The greedy scheme can obtain the best results, while the classical water-filling and equal power allocation scheme obtain the same results. Although the modified water-filling power allocation scheme can not achieve the best results, its simple implementation can win its application in TDD/TDMA 4G systems.

Finally, as showed in Fig.11, the corresponding BER results of above system configuration with requirement of BER<10^{-3}, is given by simulating the TDD/TDMA link performance through Matlab 7.0 simulink blocksets. Similar conclusion can be figured out as showed in Fig.9.

6 Conclusions

For fast fading frequency selective channels, a novel 4G cellular systems with TDD and TDMA is designed to reduce channel estimation overhead and avoid MUD algorithms with larger number of users in current 4G schemes, such as VSF-OFCDM, TDD-MIMO-OFDM, TDD-CDM-OFDM, and so on. Based on TDD/TDMA, the structures of PHY radio frame, data burst, and synchronization, are elaborately designed under the limitation of 4G system requirements. Furthermore, the construction of training sequences for Stainer channel estimation also is detailed with the novel eigenmodes coupled with universal space-time codes. Finally, the system architecture of TDD/TDMA 4G system is given and evaluated by numerical simulations. Results show that TDD/TDMA 4G systems can achieve the expectation of 4G cellular systems.

Reference:

[1] Foschini GJ, Gans MJ. On limits of wireless communications in a fading environment when using multiple antennas. *Wireless Pers. Commun.*, Vol. 6, No. 3, 1998, pp. 311–335.

[2] Holter B. On the Capacity of the Mimo Channel—A Tutorial Introduction. Dept. Telecommun., Norwegian Univ. Sci. Technol., Stavenger, Norway, *Tech. Rep.*, 2001.

[3] van Zelst A, Schenk T.C.W., Implementation of a MIMO OFDM-based wireless LAN system. *IEEE Transactions on Signal Processing*, Vol. 52, No. 2, 2004, pp. 483-494.

[4] Nanda S., Walton R., Ketchum J., Wallace M., et al. A high-performance MIMO OFDM wireless LAN. *IEEE Communications Magazine*, Vol. 43, No. 2, 2005, pp.101-109.

[5] Bin Xia, Jiangzhou Wang, Sawahashi M. Performance comparison of optimum and MMSE receivers with imperfect channel estimation for VSF-OFCDM systems. *IEEE Transactions on Wireless Communications*, Vol. 4, No. 6, 2005, pp. 3051-3062.

[6] Kishiyama Y, Maeda N., Higuchi K., et al. Transmission performance analysis of VSF-OFCDM broadband packet wireless access based on field experiments in 100-MHz forward link. *Proceedings of IEEE 60th Vehicular Technology Conference*, Vol. 5, 2004, pp. 3328-3333.

[7] Quek T.Q.S., Maeda N., Atarashi H., Sawahashi M. Analysis on tradeoff between frequency diversity and inter-code interference considering fading correlation in forward link for VSF-OFCDM wireless access. *Proceedings of IEEE 2004 60th Vehicular Technology Conference*, Vol. 2, 2004, pp. 875 – 879.

[8] Ping Zhang, Xiaofeng Tao, Jianhua Zhang, et al. A vision from the future: beyond 3G TDD. *IEEE Communications Magazine*, Vol. 43, No. 1, 2005, pp. 38-44.

[9] Guangyi Liu, Xiantao Liu, Wenguang Tian, et al. Capacities of two uplink speech schemes for FuTURE B3G TDD system in multi-cell scenario. *Proceedings of IEEE 2005 62nd Vehicular Technology Conference*, Vol. 3, 2005, pp. 1489 – 1493.

[10] Yin Changchuan, Zhao Xueyuan, Hou Xiaolin, et al. A Simulation Study on Channel Estimation for MIMO-OFDM Based Beyond 3GMobile Systems. *The Journal of China Universities of Posts and Telecommunica*, Vol. 12, No. 3, 2005, pp. 7-11.

[11] Xiaofeng Tao, Jin Xu, Xiaodong Xu, et al. Group Cell FuTURE B3G TDD System. *Proceedings of IEEE 16th International Symposium on Personal, Indoor and Mobile Radio Communications*, Vol. 2, 2005, pp. 967-971.

[12] Kan Zheng, Lin Huang, Wenbo Wang, Guiliang Yang. TD-CDM-OFDM: Evolution of TD-SCDMA toward 4G. *IEEE Communications Magazine*, vol. 43, no. 1, pp. 45-52, Jan. 2005.

[13] Yang Yudong, Li Fangwei. Evolution of TD-SCDMA toward TD-CDM-OFDM.

Communications World Weekly, No. 3, 2006, pp. 35-36.

[14] Yang Yudong, Li Fangwei. TD-SCDMA Column TD-CDM-OFDM: The Next Generation TD-SCDMA. *Modern Science & Technology of Telecommunications*, No. 3, 2006 pp. 51-53+69.

[15] Myung-Sun Baek, Hyung-Joon Kook, Mi-Jeong Kim, et al. Multi-antenna scheme for high capacity transmission in the digital audio broadcasting. *IEEE Transactions on Broadcasting*, Vol. 51, No.4, 2005, pp. 551-559.

[16] Biguesh M., Gershman A.B. Training-Based MIMO Channel Estimation: A Study of Estimator Tradeoffs and Optimal Training Signals. *IEEE Transactions on Signal Processing*, Vol. 54, No. 3, 2006, pp. 884-893.

[17] Ogawa Y., Nishio K., Nishimura T., Ohgane T. Channel and frequency offset estimation for a MIMO-OFDM system. *Proceedings of IEEE 60th Vehicular Technology Conference,* Vol. 2, 2004, pp. 1523-1527.

[18] Steven M Kay. *Fundamental of statistical signal processing volume I: estimation Theory*, Prentice Hall PTR, 1999.

[19] User Equipment (UE) radio transmission and reception (TDD), 3GPP TS 25.102.720, *http://www.3gpp.org/ftp/Specs/ archive/25_series/25.102/25102-720.zip* ,2006-7-6

[20] Rappaport TS, *Wireless Communications Principles and Practice, Second Edition*, Prentice Hall PTR, Upper Saddle River, NJ. 2002.

[21] OFDM System Design Example:Indoor Wireless LAN, *http://ee.eng.usf.edu /gradcourses/EE-seminar/presentations/nezami-2.pdf*, 2006-8-8

[22] Channel models for fixed wireless applications, *http://www.ieee802.org/16/tga/docs/80216a-03_01.pdf*, 2006/4/25

[23] Method and Principle of Uplink Synchronization, *http://www.3gpp.org/ftp /tsg_ran/WG1_RL1/TSGR1_05/ Docs/Pdf/ r1-99624.pdf*, 2006/5/18

[24] 3rd Generation Partnership Project; *Technical Specification Group Radio Access Network;Physical channels and mapping of transport channels onto physical channels (TDD) (Release 7)*, 3GPP TS 25.221 V7.0.0 (2006-03).

[25] Schmidl T.M., Cox D.C., "Robust frequency and timing synchronization for OFDM", *IEEE Transactions on Communications,* vol. 45, no. 12, pp. 1613-1621, Dec. 1997.

[26] Ogawa Y., Nishio K., Nishimura T., Ohgane T., A MIMO-OFDM system for high-speed transmission. *Proceedings of IEEE 2003 58th Vehicular Technology Conference*, Vol. 1, 2003, pp. 493-497.

[27] Dmitry Kramarev, Insoo Koo, Kiseon Kim. An Approximated Detection Method for Sequential Detection in Wireless Sensor Networks. *Proceedings of the 11th WSEAS International Conference on COMMUNICATIONS*, 2007, pp. 260-265.

[28] Quoting Lai, Junxun Yin, Fan Lin, et al, Performance of adaptive bit and power allocation MIMO-OFDM system based on greedy algorithm, *Proceedings of 2005 International Conference on Networking and Mobile Computing,* Vol. 1, 2005, pp.44-49.

[29] Telatar E., Capacity of multi-antenna Gaussian channels, *European Transactions on Telecommunications*, Vol. 10, No. 6, 1999, pp. 585–595.

[30] Nanda S., Walton R., Ketchum J., et al., A high-performance MIMO OFDM wireless LAN, *IEEE Communications Magazine*, Vol. 43, No. 2, 2005, pp. 101-109.

[31] Diaz J., Bar-Ness Y., Ye Hoon Lee, A New Approach to Joint AMC and Power Allocation for MIMO-OFDM, *Proceedings of 2006 International Conference on Internet and Web Applications and Services/Advanced International Conference on Telecommunications*, 2006, pp. 38-42.

[32] Thomas M.Wendt, Leonhard M, Reindl, Reduction of Power Consumption in Wireless Sensor Networks through Utilization of Wake up Strategies, *Proceedings of the 11th WSEAS International Conference on SYSTEMS*, 2007, pp. 255-258.